Unlocking the Potential of Ni-rich NCM811 Cathodes: Chlorine Substitution as a Pathway to Prevent Oxygen Release and Transition-Metal Dissolution

Santhanamoorthi Nachimuthu[a,†], Shi-Hong Xu[a,†], Ryo Maezono[b, c], Bing Joe Hwang [d, e, f], and Jyh-Chiang Jiang [a, f,*]

[a]Computational and Theoretical Chemistry Laboratory, Department of Chemical Engineering, National Taiwan University of Science and Technology, Taipei 10607, Taiwan

[b]School of Information Science, Japan Advanced Institute of Science and Technology (JAIST), Nomi, Ishikawa 923-1292, Japan

[c]Graduate Major in Materials and Information Sciences, Institute of Science Tokyo, 2-12-1-S6-22 Ookayama, Meguro-ku, Tokyo 152-8550, Japan

[d]Department of Chemical Engineering, National Taiwan University of Science and Technology, Taipei 10607, Taiwan

[e]National Synchrotron Radiation Research Center (NSRRC), Hsinchu 30076, Taiwan

[f]Sustainable Electrochemical Energy Development Center, National Taiwan University of Science and Technology, Taipei 106, Taiwan

*Corresponding author Email: jcjiang@mail.ntust.edu.tw
Telephone: +886-2-27376653. Fax: +886-2-27376644
† First authors contributed equally to this work

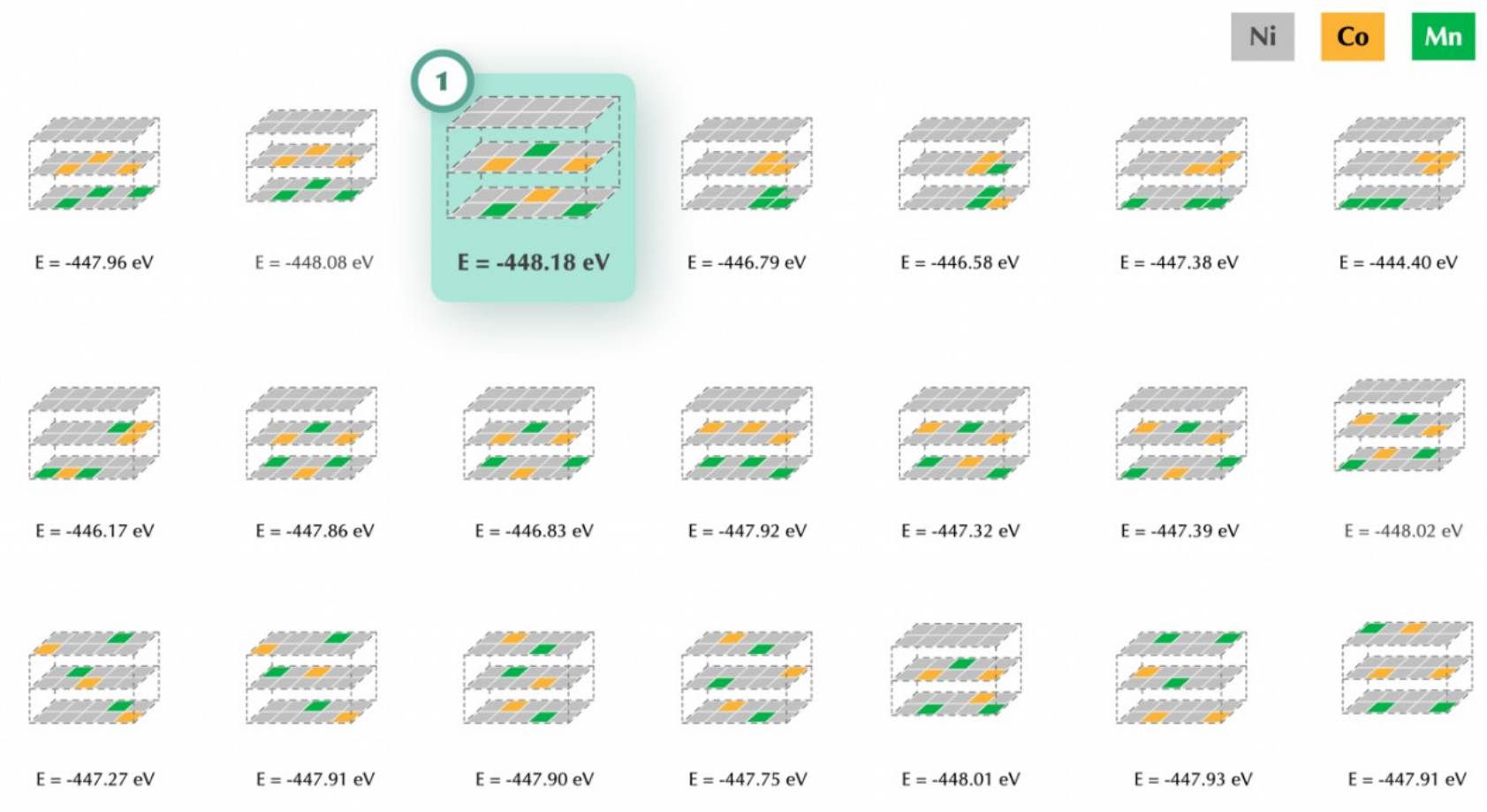

Figure S1. Schematic representation of possible bulk NCM811 configurations derived from $LiNiO_2$, showing different Co and Mn substitutional arrangements at Ni sites. The corresponding total energies of these configurations are also shown.

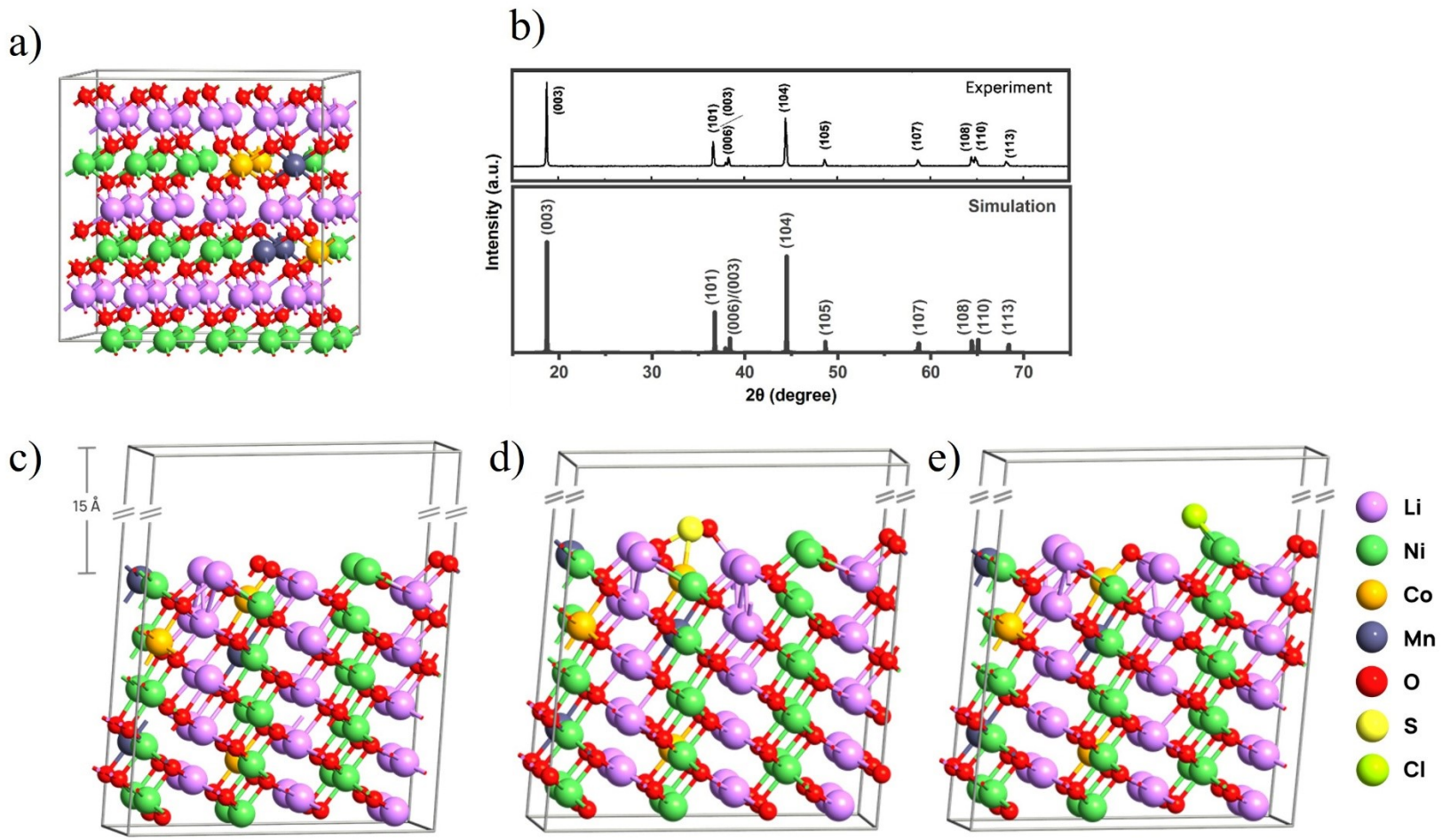

Figure S2. (a) Optimized structure of the most thermodynamically stable bulk NCM811 unit cell, (b) simulated and experimental XRD patterns of NCM811, (c) most stable termination of the pristine NCM811 (006) surface, (d) S-doped NCM811 surface, (e) Cl-doped NCM811 surface.

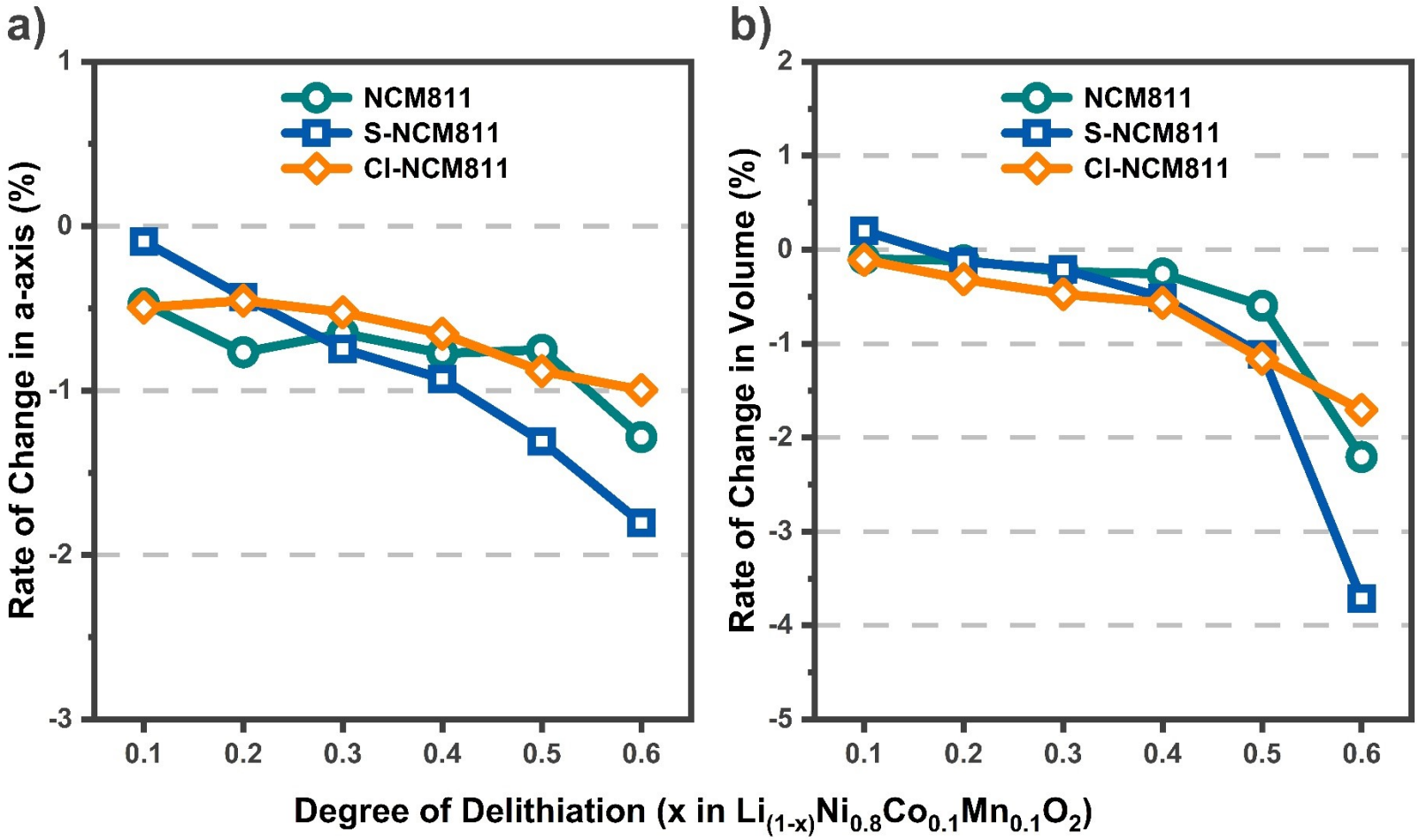

Figure S3. Rate of change (ROC) in (a) the in-plane lattice parameter *a* and (b) the unit cell volume of pristine NCM811, S-NCM811, and Cl-NCM811 surfaces as a function of delithiation.

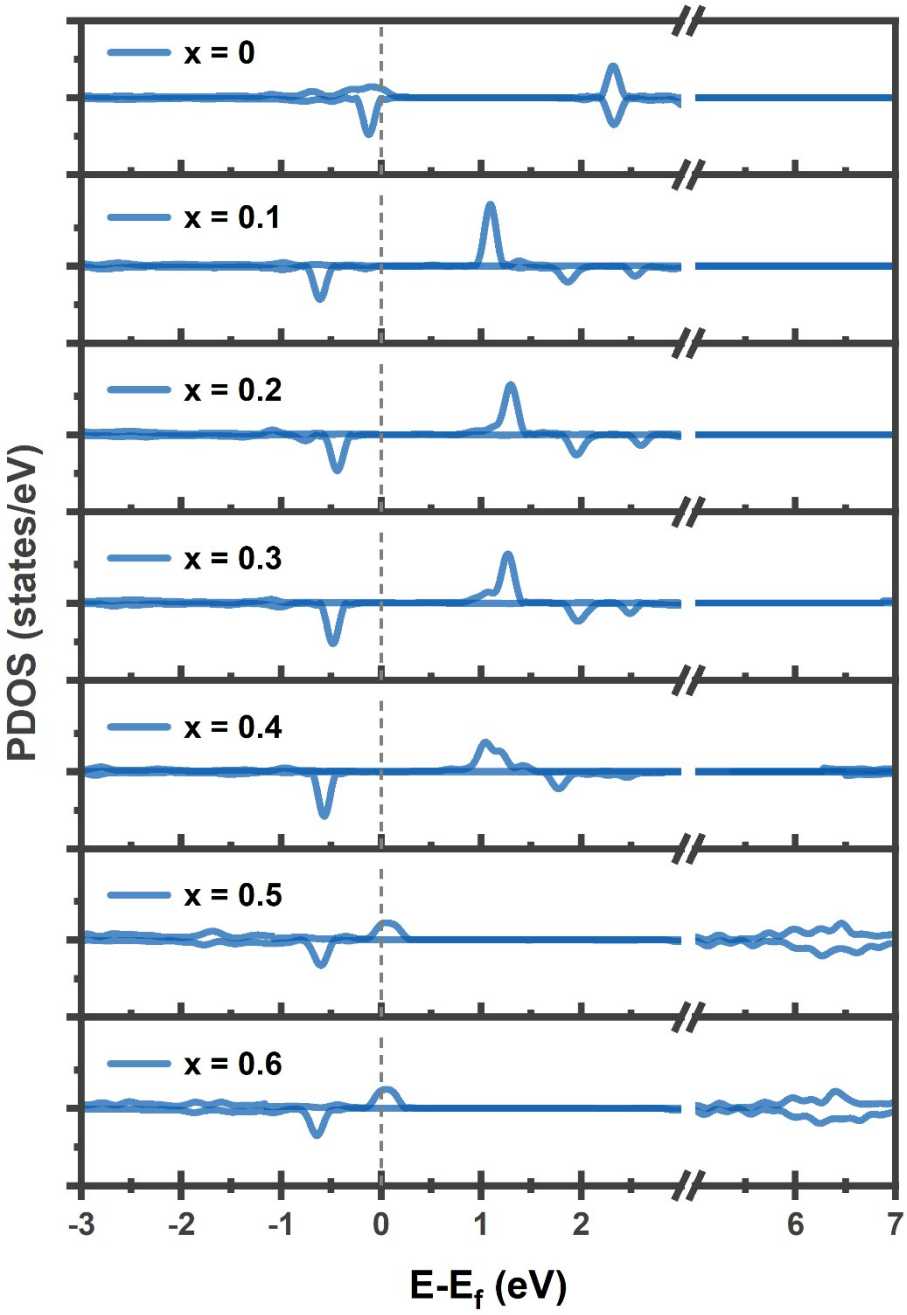

Figure S4. Projected density of states (PDOS) of the S p-orbital in the S-NCM811 surface at delithiation levels from x = 0 to x = 0.6. The vertical dashed line represents the Fermi level.

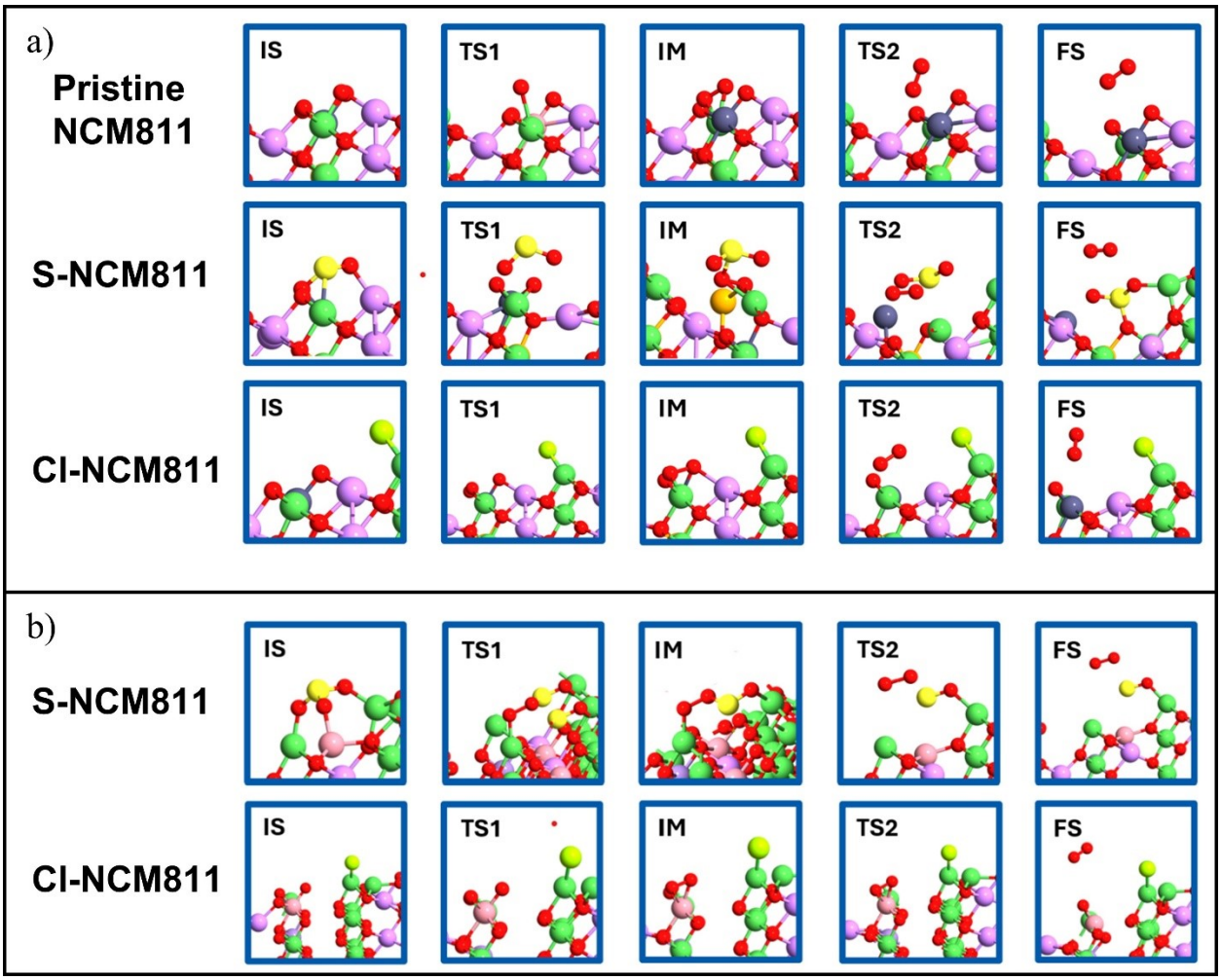

Figure S5. Snapshots of intermediate structures during O_2^- formation and O_2 release on NCM811 surfaces: (a) Pristine NCM811, S-NCM811, and Cl-NCM811 surfaces at a delithiation level of x = 0.3, and (b) S-NCM811 and Cl-NCM811 surfaces at a delithiation level of x = 0.6.

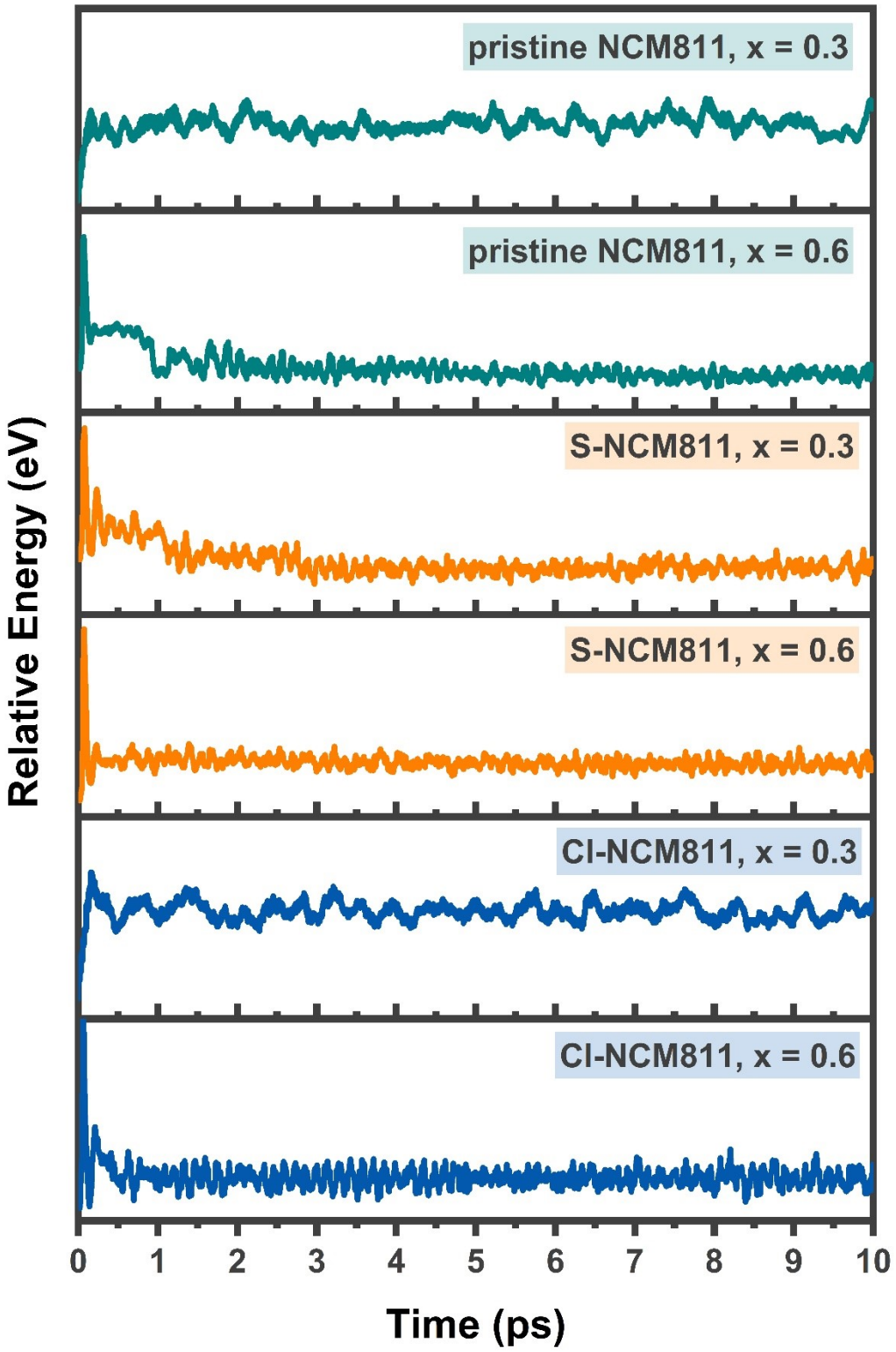

Figure S6. Relative total energy as a function of simulation time from AIMD for pristine, S-NCM811, and Cl-NCM811 surfaces at delithiation levels of x = 0.3 and x = 0.6.

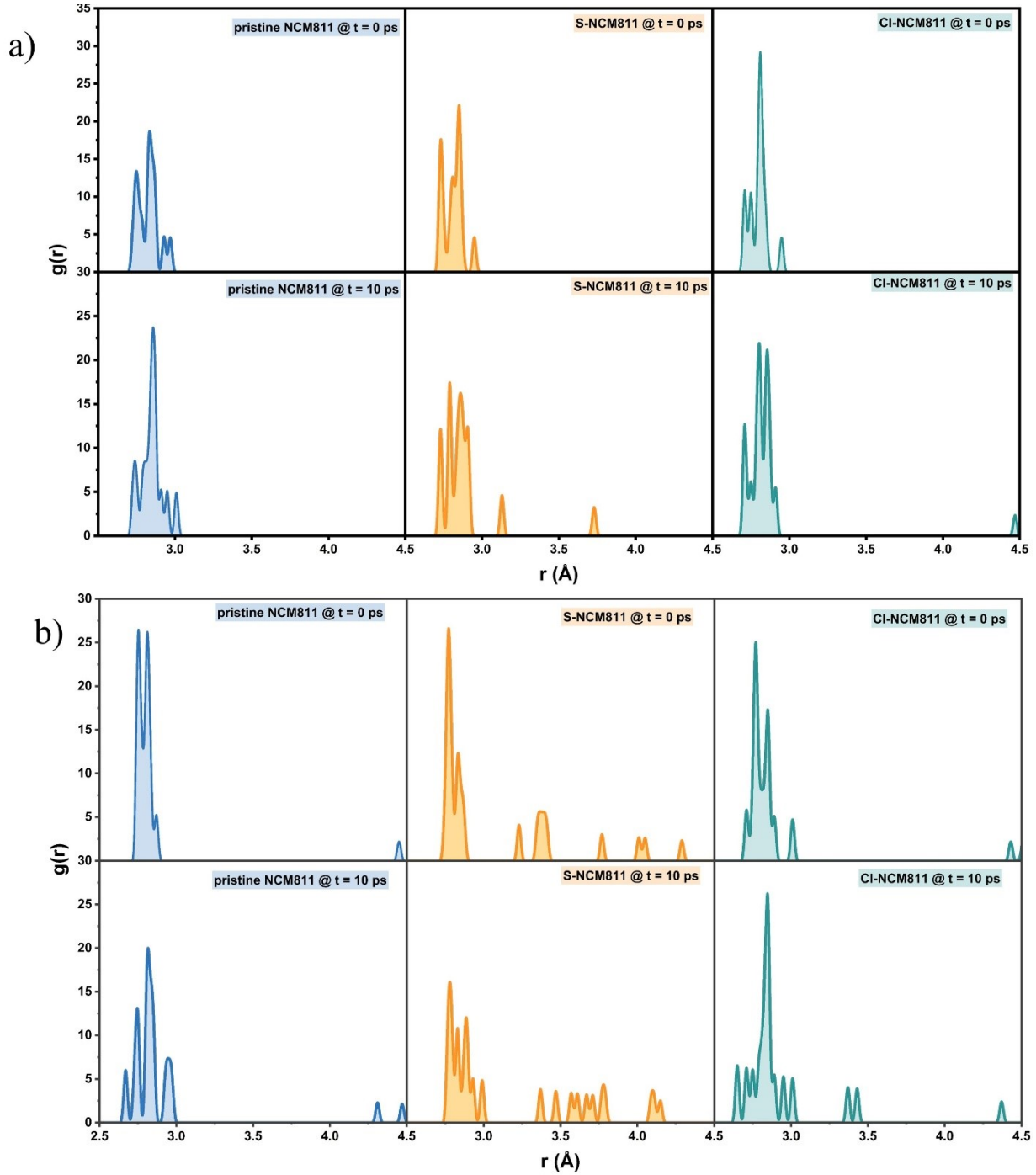

Figure S7. RDFs of Co-Ni pairs in pristine, S-NCM811, and Cl-NCM811 surfaces at delithiation levels of (a) x = 0.3 and (b) x = 0.6, shown at the initial (t = 0 ps) and final (t = 10 ps) stages of the AIMD simulations.

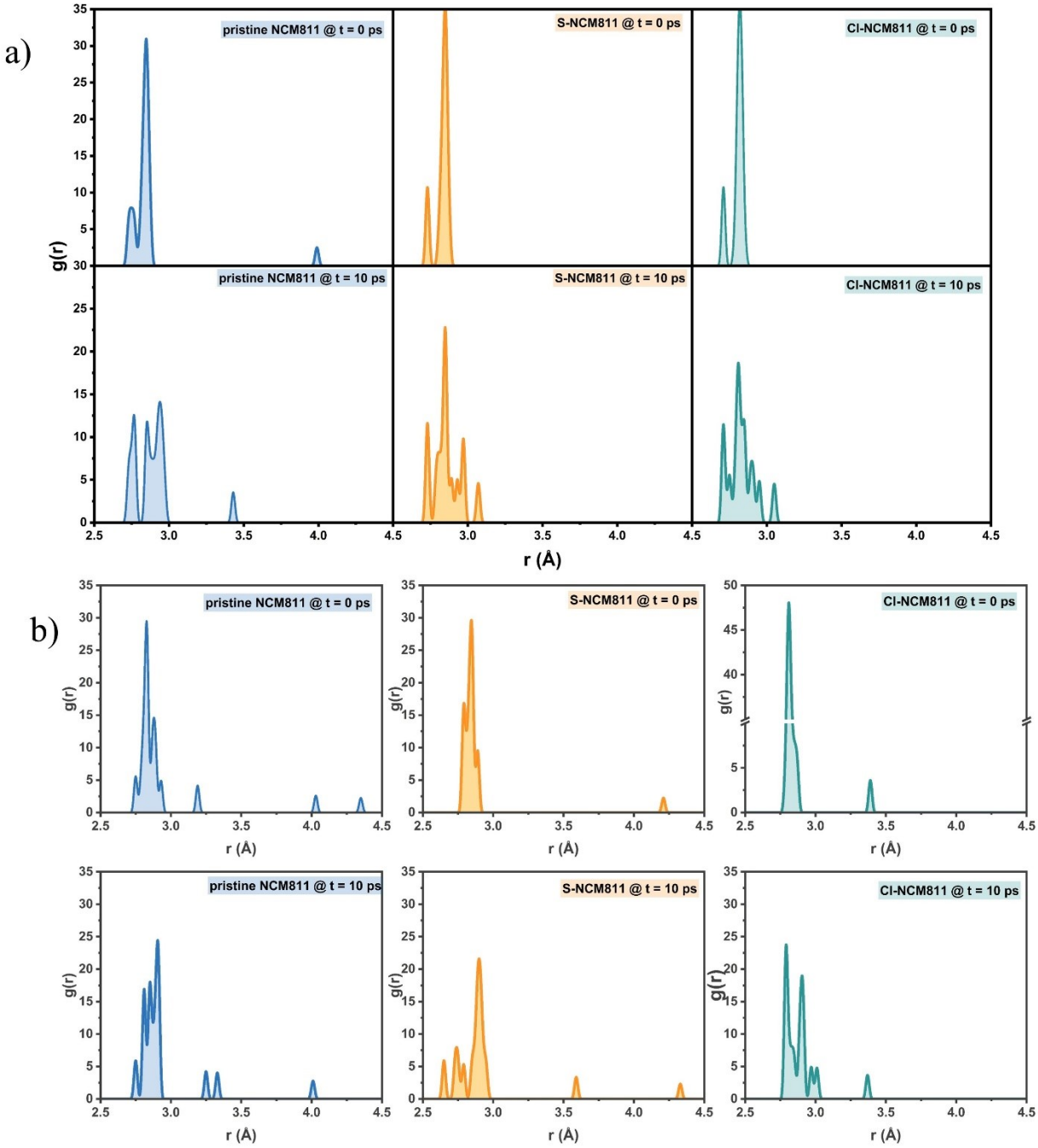

Figure S8. RDFs of Mn-Ni pairs in pristine, S-NCM811, and Cl-NCM811 surfaces at delithiation levels of (a) x = 0.3 and (b) x = 0.6, shown at the initial (t = 0 ps) and final (t = 10 ps) stages of the AIMD simulations.

Table S1. Oxidation states and corresponding magnetic moments of transition metals.

Species	Magnetic moment (μB)
Ni^{2+}	1.75
Ni^{3+}	1.15
Ni^{4+}	0.11
Co^{3+}	-0.04
Co^{4+}	-1.32
Mn^{4+}	-3.32

Table S3. Distribution of Ni^{2+}, Ni^{3+}, and $Ni4^{+}$ species in the top two layers of pristine and Cl-NCM811 surfaces at delithiation levels of x = 0 and x = 0.5

Pristine NCM811	**x = 0**			**x = 0.5**		
	Ni^{2+}	**Ni^{3+}**	**Ni^{4+}**	**Ni^{2+}**	**Ni^{3+}**	**Ni^{4+}**
Ni	4	4	0	1	4	3
Cl-NCM811						
Ni coordinated with Cl	3	1	0	4	0	0
Ni not coordinated with Cl	0	4	0	0	2	2

Table S2. Oxidation states of Co and Mn in pristine and anion-doped NCM811 at different delithiation levels.

Delithiation Level (x)	Pristine NCM811							S-NCM811							Cl-NCM811						
	0.0	**0.1**	**0.2**	**0.3**	**0.4**	**0.5**	**0.6**	**0.0**	**0.1**	**0.2**	**0.3**	**0.4**	**0.5**	**0.6**	**0.0**	**0.1**	**0.2**	**0.3**	**0.4**	**0.5**	**0.6**
Mn1	+4	+4	+4	+4	+4	+4	+4	+4	+4	+4	+4	+4	+4	+4	+4	+4	+4	+4	+4	+4	+4
Mn2	+4	+4	+4	+4	+4	+4	+4	+4	+4	+4	+4	+4	+4	+4	+4	+4	+4	+4	+4	+4	+4
Mn3	+4	+4	+4	+4	+4	+4	+4	+4	+4	+4	+4	+4	+4	+4	+4	+4	+4	+4	+4	+4	+4
Co1	+3	+3	+3	+3	+3	+3	+3	+3	+3	+3	+3	+3	+4	+4	+3	+3	+3	+3	+3	+3	+3
Co2	+3	+3	+3	+3	+3	+4	+4	+3	+3	+3	+3	+3	+4	+4	+3	+3	+3	+3	+3	+4	+4
Co3	+4	+4	+4	+4	+4	+4	+4	+3	+4	+4	+4	+4	+4	+4	+4	+4	+4	+4	+4	+4	+4